

See discussions, stats, and author profiles for this publication at: <https://www.researchgate.net/publication/13757388>

On Numerical Simulations of Integrate-and-Fire Neural Networks

Article in *Neural Computation* · March 1998

DOI: 10.1162/089976698300017845 · Source: PubMed

CITATIONS

168

READS

500

4 authors, including:



David Hansel

Paris Descartes, CPSC

133 PUBLICATIONS 5,432 CITATIONS

[SEE PROFILE](#)



German Mato

Centro Atómico Bariloche

64 PUBLICATIONS 2,008 CITATIONS

[SEE PROFILE](#)



Claude Meunier

Paris Descartes, CPSC

56 PUBLICATIONS 1,848 CITATIONS

[SEE PROFILE](#)

Some of the authors of this publication are also working on these related projects:



Motoneurons [View project](#)



Dynamics and Plasticity in Cortex [View project](#)

On numerical simulations of integrate-and-fire neural networks

D. Hansel (1), G. Mato (2), C. Meunier (1) and L. Neltner (1)

(1) Centre de Physique Théorique UPR014 CNRS

Ecole Polytechnique 91128 Palaiseau Cedex, France,

(2) Centro Atómico Bariloche

Comisión Nacional de Energía Atómica, 8400 S. C. de Bariloche, Argentina

Abstract

It is shown that very small time steps are required to correctly reproduce the synchronization properties of large networks of integrate-and-fire neurons when the differential system describing their dynamics is integrated with the standard Euler or second order Runge-Kutta algorithms. The reason for that behavior is analyzed and a simple improvement of these algorithms is proposed.

1 Introduction

Our theoretical understanding of the properties of large neuronal systems relies heavily on simulations of networks consisting of up to several thousands interacting neurons. Such simulations are highly time consuming: for a general network architecture, the CPU time is dominated by the evaluation of the interactions between neurons and scales like N^2 , where N is the size of the network. Moreover, one frequently needs to investigate the system's behavior for many different sets of parameters or to perform a statistical analysis over many initial conditions or samples of the internal noise. It is therefore crucial to integrate the dynamics with an appropriate algorithm, that allows one to use as large a time step as possible.

Integrate-and-fire (IF) neurons are frequently used for modeling networks of interacting neurons. In IF models, the active properties of the neural membrane responsible for spike generation are not explicitly taken into account. Only the passive membrane properties are incorporated in the equations and one assumes that a spike is fired whenever the membrane potential of the neuron crosses some prescribed threshold. In the simplest IF model (Lapicque 1907, Tuckwell 1988), this firing is followed by the instantaneous resetting of the membrane potential at its resting value. In other models, a potassium conductance opens at firing time, that leads to the repolarization of the membrane potential (see for instance Wehmeier et al., 1989, for a large scale neural network using such a model). These passive IF models are less steep than the biophysically more realistic conductance-based models, which incorporate the fast voltage dependent ionic currents responsible for the firing of action potentials (Hodgkin and Huxley, 1952), and it seems that larger time steps could be used to integrate stably their dynamics. However, the IF dynamics presents discontinuities of the membrane potential or its derivatives at firing times which may cause severe numerical problems. This has led several authors to use “exact integration schemes” (Tsodyks et al., 1993, Mascagni and Sherman, 1997), that are easily written for Lapicque neurons interacting through synaptic currents and run reasonably fast. However, such schemes cannot be extended to any IF model or to interactions described by synaptic conductances. A number of questions thus remain open, regarding the numerical integration of IF models. Under which conditions, in particular for which time steps, can reliable results be obtained when a simple integration scheme, such as the Euler algorithm or the second order Runge Kutta algorithm (hereafter RK2) is used? Can other numerical schemes avoid the problems due to discontinuities without jeopardizing the computational efficiency? These issues are addressed in the present report in the framework of large globally coupled networks of identical IF neurons.

The paper is organized as follows. In the next section we describe the IF network model used

in this study, explain how the level of synchrony of the network can be characterized and how we estimate the error on the numerical integration of the dynamics. In Section 3 we show that very small time steps are needed to correctly integrate the dynamics of an IF network when the Euler algorithm is used. We also show that using schemes that are a priori of higher order, such as the RK2 algorithm, does not help, as the global integration error is dominated by errors arising from the discontinuous nature of the dynamics. We then demonstrate that the addition of a simple interpolation scheme at firing times allows us to solve these problems. Finally Section 4 is devoted to the summary and discussion of our results.

2 Methods

2.1 The model

We consider a network of $N = 128$ identical excitatory neurons. For the sake of simplicity, we assume that the neurons are coupled all-to-all. Neurons are described by a single compartment integrate-and-fire model. The membrane potential evolves in the passive zone below the firing threshold θ according to the linear differential equation:

$$C \frac{dV}{dt} = -g_l(V - V_l) + I_{syn}(t) + I_0 \quad (1)$$

where g_l and V_l are the conductance and the reversal potential of the voltage-independent leak current, I_{syn} is the synaptic current due to the action of the other neurons of the network. The current I_0 is a constant external drive, that makes the neurons fire periodically when uncoupled. The membrane capacitance C is set at $1 \mu F/cm^2$. Requiring a passive membrane time constant $\tau = C/g_l$ of 10 ms leads to a leak conductance $g_l = 0.1 \text{ mS/cm}^2$.

The resting membrane potential $V_{rest} = V_l$ is equal to -60 mV in our simulations. Whenever the membrane potential V reaches the threshold θ (-40 mV in our simulations) a spike is fired and V is instantaneously reset to rest:

$$V(t_0^+) = V_{rest} \quad \text{if} \quad V(t_0^-) = \theta \quad (2)$$

We do not incorporate any absolute refractory period in the dynamics.

When the change in the membrane conductance due to synaptic interactions is not taken into

account, the synaptic current $I_{syn}(t)$ is given by

$$I_{syn}(t) = \frac{\bar{I}_{syn}}{N} \sum_{neurons} \sum_{spikes} f(t - t_{spike}) \quad (3)$$

where

$$f(t) = \frac{1}{\tau_1 - \tau_2} \left(e^{-\frac{t}{\tau_1}} - e^{-\frac{t}{\tau_2}} \right) \quad (4)$$

The summation is performed over all the spikes emitted prior to time t by all the other neurons of the network. The normalization adopted here ensures that the time integral of $f(t)$ is always unity.

For such an interaction, that is used throughout the paper with synaptic time constants $\tau_1 = 3 \text{ ms}$ and $\tau_2 = 1 \text{ ms}$, one can write closed analytical expression for the evolution of the membrane potentials of the neurons during time intervals where no spike is fired in the network. Another and biophysically more realistic description of the synaptic current can also be used that incorporates changes in the membrane conductance:

$$I_{syn}(t) = -g_{syn}(V - V_e) \sum_{neurons} \sum_{spikes} f(t - t_{spike}) \quad (5)$$

where $f(t)$ has the same form as in Eq. (4) and V_e is the reversal potential of the synaptic current. A closed expression can still be derived for V but it must now be evaluated by numerical integration.

2.2 Initial conditions

At $t = 0$, all synaptic currents are set to 0 and the potentials of the neurons are chosen according to:

$$V_i(0) = \tau I_0 + (V_{rest} - \tau I_0) \exp\left(-c \frac{i-1}{N} \frac{T}{\tau}\right) \quad (6)$$

($i = 1, \dots, N$), where

$$T = -\tau \ln\left(\frac{\tau I_0 - \theta}{\tau I_0 - V_{rest}}\right) \quad (7)$$

is the firing period of the neurons in the absence of interaction, and the coefficient $0 < c < 1$ controls the degree of synchrony of the initial condition. Setting $c = 0$ yields a perfectly synchronized initial condition. On the other hand, $c = 1$ corresponds to an uniform distribution of firing times for uncoupled neurons.

2.3 Measure of synchrony

To measure the degree of synchrony in the network we follow the method proposed and developed in (Hansel and Sompolinsky 1992, Golomb and Rinzel 1993, Ginzburg and Sompolinsky 1994), that is grounded on the analysis of the temporal fluctuations of the activity. One evaluates at a given time t the average membrane potential:

$$A_N(t) = \frac{1}{N} \sum_{i=1}^N V_i(t) \quad (8)$$

Its time fluctuations can be characterized by the variance

$$\Delta_N = \left\langle A_N(t)^2 \right\rangle_t - \langle A_N(t) \rangle_t^2 \quad (9)$$

This variance is normalized to the population averaged variance of single cell activity

$$\Delta = \frac{1}{N} \sum_{i=1}^N (\langle V_i(t)^2 \rangle_t - \langle V_i(t) \rangle_t^2) \quad (10)$$

The resulting coherence parameter

$$\Sigma_N = \frac{\Delta_N}{\Delta} \quad (11)$$

behaves generally for large N as

$$\Sigma_N = \chi + \frac{a}{N} + O\left(\frac{1}{N^2}\right) \quad (12)$$

where a is some constant number and χ , comprised between 0 and 1, measures the degree of coherence in the system. In particular, $\chi = 1$ if the system is totally synchronized (i.e. $V_i(t) = V(t)$ for all i) and $\chi = 0$ if the state of the system is asynchronous.

In the rest of this work, the computation of Σ_N is performed by running simulations over $t = 10$ s, and sampling the state of the network every 1 ms from time $t = 5$ s to time $t = 10$ s. The network size we use is not large enough to preclude finite size effects in the dynamical properties (see Hansel and Sompolinsky 1996, for discussions of this issue in neural modeling). However we are interested here in the accuracy in the estimate of Σ_N and not in its large size limit, and a size $N = 128$ is sufficient for this purpose. In the following, Σ_{128} will be denoted simply by Σ .

2.4 Exact integration and estimate of the numerical error in a simulation

We first recall how the model defined by Eq. (1-4) can be integrated exactly. Solving Eq. (1) for the membrane potential one finds:

$$V_i(t) = V_i(0)e^{-t/\tau} + \frac{I_0}{g_l}(1 - e^{-t/\tau}) + V_l(1 - e^{-t/\tau}) + \int_0^t e^{(t'-t)/\tau} \frac{I_{syn}(t')}{C} dt' \quad (13)$$

($i = 1, \dots, N$) where the first three terms correspond to the single cell dynamics and the last term stems from synaptic interactions.

Since $I_{syn}(t')$ is a combination of exponential functions, the integral in the last term can be computed analytically. Starting from a given state of the network and a given value of the synaptic current, one uses Eq. (13) to calculate the first time at which a neuron fires. The potential of that neuron is then reset to rest, the membrane potential of the other neurons is evaluated and a new spike is included in Eq. (3). This procedure is then iterated again and again. In this method, integrating the differential equations amounts to solving transcendental equations. This can be done at an arbitrary desired precision within the limits of computer accuracy, by using for instance a Newton-Raphson scheme, hence the name of “exact method”. This method has been used by Tsodyks et al. (1993) to study the synchronization properties of IF networks. The results it gives will be used as a comparison point for the results we obtain with different algorithms.

In the following, we will evaluate the accuracy of the numerical integration of the network dynamics, by computing the error on the timing of the last 50 spikes of each neurons. More precisely, we use the quantity:

$$\epsilon_t = \frac{f}{50N} \sum_{i=1}^N \sum_{j=1}^{50} |\hat{t}_i(n_i - j) - t_i(n_i - j)| \quad (14)$$

where n_i is the total number of spikes fired by neuron i in the run, $t_i(k)$ the exact time at which neuron i has fired its k^{th} spike, $\hat{t}_i(k)$ its numerical estimate.

We will also estimate the relative error on the average firing rate (computed between the times $t = 5$ s and $t = 10$ s) of the whole population:

$$\epsilon_f = \left| \frac{\hat{f} - f}{f} \right| \quad (15)$$

and the relative error on the coherence:

$$\epsilon_\Sigma = \left| \frac{\hat{\Sigma} - \Sigma}{\Sigma} \right| \quad (16)$$

Here f and Σ represent the exact values of the firing rate and the coherence, while \hat{f} and $\hat{\Sigma}$ are the numerical estimates of these quantities.

3 Results

3.1 Euler algorithms

3.1.1 Standard Euler algorithm

The Euler scheme with fixed time step is the simplest integration scheme that can be used to study the dynamics of the network. Knowing the membrane potential and the synaptic conductance at time t one calculates the membrane potential at time $t + \Delta t$ according to:

$$V(t + \Delta t) = V(t) + \Delta t(-g_l(V(t) - V_l) + I_{syn}(t) + I_0) \quad (17)$$

When $V(t + \Delta t) > \theta$, a spike is assumed to be fired at time $t + \Delta t$ and the membrane potential is reset. Synaptic conductances are then updated accordingly.

Fig. 1 displays the coherence Σ of the network as a function of the synaptic strength \bar{I}_{syn} for $\Delta t = 0.25 \text{ ms}$, $\Delta t = 0.1 \text{ ms}$ and $\Delta t = 0.01 \text{ ms}$. We have also plotted on the same graph the results yielded by an exact integration. In all these simulations the initial condition was partially coherent ($c = 0.5$, see section 2.2). At large time, the exact value of the coherence is a decreasing function of the synaptic strength in agreement with the fact that excitation is desynchronizing for integrate-and-fire neurons (Hansel et al. 1995, Van Vreeswijk et al. 1995). At large coupling the network is in the incoherent state and accordingly the synchrony is of order $O(\frac{1}{N})$. The synchronization transition occurs for $\bar{I}_{syn} \approx 0.78 \mu A/cm^2$.

The curve obtained for a time step $\Delta t = 0.25 \text{ ms}$ deviates strongly from the exact result in all the range of coupling strength. Moreover, as shown in Fig. 2, the numerical estimate of the coherence depends on the initial conditions of the network. For $\Delta t = 0.1 \text{ ms}$ some improvement is seen but, again, the results depend on the initial conditions. Moreover the synchrony parameter does not display the correct qualitative behavior at small coupling and the location of the transition is incorrectly predicted. This latter problem is alleviated with a time step of $\Delta t = 0.01 \text{ ms}$ but the coherence in the region of large synchrony does not yet behave smoothly and still differs from the exact value by 15 – 20%. An integration time step of $\Delta t = 0.001 \text{ ms}$ is actually required to evaluate correctly the coherence of the network in this regime (result not shown). The firing rate

of the network, evaluated with the exact method, varies from $f \approx 50 \text{ Hz}$ at weak coupling to $f \approx 90 \text{ Hz}$ near the transition. Therefore, the minimum time step required to describe correctly the synchronization properties corresponds to $O(10^4)$ time steps per firing period.

The order of the integration algorithm can be derived from the errors ϵ_f and ϵ_t on the firing rate and on the timing of the spikes at different integration time steps. The results are displayed in Fig. 3-5 (full line). Here the synaptic strength has been fixed to $\bar{I}_{syn} = 0.60 \mu\text{A}/\text{cm}^2$, in the midst of the synchronized phase.

For sufficiently small time steps, ϵ_t and ϵ_f go to zero linearly in the time step. A fit of the results yields:

$$\epsilon_t^E = A_t^E \Delta t \quad (18)$$

with $A_t^E \approx 242 \text{ ms}^{-1}$, and

$$\epsilon_f^E = A_f^E \Delta t \quad (19)$$

with $A_f^E \approx 24.4 \text{ ms}^{-1}$.

The relative error on the coherence is plotted in Fig. 5. It decreases to zero linearly with the time step, although the scaling is not as precise as for ϵ_f and ϵ_t . This can be explained by the discontinuity inherent to IF neurons. Indeed, it may happen that, at sampling time, some neurons are very close to the firing threshold. Depending on the time step, the numerically estimated value of the potential for these neurons will be either close θ (the neuron is about to fire) or close to V_{rest} (the neuron has just fired). This introduces irregularities in the scaling behavior that would not be met for a model with a continuous evolution of the potentials. We have checked that last point by simulating a network of IF neurons, the dynamics of which incorporates an AHP current, which led to a much better scaling for the coherence Σ .

These results show that although the Euler algorithm is a first order integration scheme and converges to the correct results in the limit $\Delta t \rightarrow 0$, very small time steps, compared to the firing period, are required to achieve a reasonable precision (see also Tables 1 and 2).

3.1.2 Improved Euler algorithm

The standard Euler algorithm can be modified to increase the accuracy on the determination of firing times, by adding a linear interpolation scheme at firing times, i.e., when at time $t + \Delta t$ the potential $V_0(t + \Delta t)$ (obtained using the standard Euler algorithm) is above threshold. This interpolated value

of the firing time is then used to estimate the potential at time $t + \Delta t$, yielding

$$V(t + \Delta t) = (V_0(t + \Delta t) - \theta) \left(1 + g_l \Delta t \frac{V(t) - V_{rest}}{V_0(t + \Delta t) - V(t)} \right) + V_{rest} \quad (20)$$

and to update the synaptic current (see Appendix).

Fig. 6 displays the results of simulations performed with this algorithm. The interpolation greatly improves the performance of the integration that now yields the correct qualitative behavior of the coherence. However, small time steps are still required to achieve good quantitative results.

This modified Euler scheme is expected to be also first order in the time step. This is confirmed by Fig. 3-5. For example, the error on the timing of spikes behaves linearly:

$$\epsilon_t^{EI} = A_t^{EI} \Delta t \quad (21)$$

with $A_t^{EI} \approx 169 \text{ ms}^{-1}$. Note that the prefactor is about 30% smaller than for the standard Euler algorithm.

3.1.3 Estimate of the error introduced by the discontinuity of the dynamics

The improvement in accuracy achieved with a linear interpolation originates in the elimination from the global error of a term of order $O(\Delta t)$ due to the discontinuity of the dynamics. When a neuron fires a spike between times t and $t + \Delta t$, a local error on the firing time of order $O(\Delta t)$ is made in the standard algorithm, which assumes that firing occurs systematically at time $t + \Delta t$. This has two consequences. First, it leads to an error of order $O(\Delta t)$ on the value of the potential at time $t + \Delta t$. The frequency of occurrence of such errors depends on the firing rate but not on the time step. Their contribution to the global error is then of order $O(\Delta t)$. But the error on the firing time also introduces an error of order $O(\Delta t)$ on the interaction term which itself produces at each time step an error on the potential of the neurons of order $O(\Delta t^2)$ and leads to a global error of order $O(\Delta t)$. So, the global error of order $O(\Delta t)$ is comprised of two terms: the former is directly related to the resetting and persists in the case of a single neuron, while the latter is mediated by the interaction and exists only in networks. Using a linear interpolation scheme enables one to increase the order in Δt of both error terms as the firing times are then estimated with a precision of $O(\Delta t^2)$.

The results of the previous section indicate that the error in the standard Euler algorithm stemming from the discontinuity of the dynamics is for small Δt of the same order of magnitude as the error due to the integration between firing times. More precisely, a lower bound for the importance

of the error induced by the discontinuity of the dynamics is given by the quantity:

$$\epsilon_t^{reset} = \epsilon_t^E - \epsilon_t^{EI} \approx 73\Delta t \quad (22)$$

3.2 Second order Runge-Kutta algorithms

One might think that reliable results can be obtained for a larger time step and without relying on an interpolation by increasing the order of the discretization in time. If one uses for instance the standard second order Runge-Kutta (RK2) algorithm, the potential is now updated according to (see for instance Mascagni and Sherman, 1997):

$$V(t + \Delta t) = V(t) + \frac{\Delta t}{2}(-g_l(V(t) + \Delta t f_1(t) - V_l) + I_{syn}(t + \Delta t) + I_0 + f_1(t)) \quad (23)$$

where

$$f_1(t) = -g_l(V(t) - V_l) + I_{syn}(t) + I_0 \quad (24)$$

and $I_{syn}(t + \Delta t)$ is computed as if no spike were emitted between t and $t + \Delta t$.

However, this is not a second order scheme in the present instance, since the error on firing times is still of order $O(\Delta t)$ (see Fig. 3-5). The error on the timing of the spikes, ϵ_t^{RK2} , behaves at small time step as:

$$\epsilon_t^{RK2} = A_t^{RK2} \Delta t \quad (25)$$

where $A_t^{RK2} \approx 66 \text{ ms}^{-1}$ as expected for a first order algorithm. Moreover the fact that

$$A_t^{RK2} \approx A_t^E - A_t^{EI} \quad (26)$$

indicates that the global error in the standard RK2 scheme is dominated by the error due to the discontinuity of the dynamics, in agreement with the analysis of section 3.1.3. Subtracting the errors is meaningful in the present case as we checked that the global errors systematically decreases when moving from the standard Euler scheme to the modified Euler scheme, and then to the RK2 algorithm.

The determination of the spiking times by linear interpolation is consistent with the order 2 of the RK2 algorithm. The firing times are estimated with a precision of $O(\Delta t^2)$ which results in an error of order $O(\Delta t^3)$ in the interaction, in agreement with the local error of the method. Therefore one expects that supplementing the standard RK2 algorithm with a linear interpolation scheme

(hereafter RK2I scheme) will yield a consistent second order algorithm for integrating IF networks. This is confirmed by figures 3-5. The quantity ϵ_t^{RK2I} now behaves as:

$$\epsilon_t^{RK2I} = A_t^{RK2I}(\Delta t)^2 \quad (27)$$

with $A_{RK2I} \approx 34 \text{ ms}^{-2}$. Moreover, this modified RK2 scheme allows one to use much larger time steps, in comparison with the previous algorithms (see Tables 1 and 2). Fig. 7 displays the coherence as a function of the coupling strength for the modified second order Runge-Kutta algorithm for $\Delta t = 0.25 \text{ ms}$, $\Delta t = 0.1 \text{ ms}$ and $\Delta t = 0.01 \text{ ms}$. The curve obtained with $\Delta t = 0.1 \text{ ms}$ is almost indistinguishable from the exact curve, whereas the numerical integration with $\Delta t = 0.25 \text{ ms}$ provides an excellent estimate in the whole range of coupling.

4 Summary and discussion

We have shown on the example of an all-to-all network of integrate-and-fire excitatory neurons that standard integration algorithms (Euler or Runge-Kutta) give reliable quantitative estimates of the synchrony properties only for very small integration time steps. A simple modification of these algorithms where the firing times are determined through a linear interpolation procedure greatly improves the integration performance. In particular, we found that time steps larger by one to two order of magnitude can be used when a modified RK2 scheme is used instead of a standard Euler or RK2 algorithm. At large time steps, standard algorithms can even lead to strong artifacts in the dynamics, under the form of *spurious multistability*. The dynamics then seems to display several asymptotic states, the state eventually reached depending on the initial condition. This originates in the fact that small differences in the firing times of different neurons are discarded when the potential is reset. Such artifacts are avoided when using a linear interpolation.

The CPU times required on a HP9000 (Model 819/K200) per time step of integration are given in table 3 for the four integration methods we compared. One iteration of the RK2 scheme takes a longer time (approximately 50 % more time) than an iteration of the Euler algorithm, as the derivative of the potential is evaluated twice per time step. Supplementing this algorithm with a linear interpolation affects very slightly this computation time and leads to an algorithm that is much more efficient than the three other integration schemes as the time step can be increased by an order of magnitude for a desired accuracy of the results. This modified algorithm is also much more efficient than the exact method. With a time step $\Delta t = 0.1 \text{ ms}$, 8.6 seconds of CPU time are required

to integrate 10 seconds of the dynamics (i.e. 10^5 time steps). In contrast the exact integration of the same 10 seconds requires about 500 seconds, a 60 fold decrease in computational efficiency. Actually even the Euler algorithm with a time step of 10^{-3} ms would be more efficient than the exact method. Note however, that when the network is composed of all-to-all coupled identical neurons, the exact method can be considerably accelerated as the neurons always fire in the same order and one can predict which neuron is going to fire next. Making use of that fact brings the exact integration on par with the modified RK2 scheme.

It is often believed that integrating the dynamics of IF networks is much faster than integrating the dynamics of similar networks of conductance based neurons. Our results show that this may not be true when a standard integration algorithm is used. On the contrary this claim is substantiated when using the RK2I algorithm.

In the IF model we have studied in this paper, we have neglected the change in membrane conductance due to synaptic interaction. This was motivated by the fact that it is then possible to compare the results obtained to those given by an exact integration scheme. However, our conclusions regarding the relative efficiency of the different algorithms are still valid when the changes in membrane conductance are taken into account, and also when a refractory period is introduced in the model.

A natural generalization of the RK2I algorithm would be a higher order Runge-Kutta methods supplemented with an interpolation scheme, that is too of higher order: a quadratic one for a third order Runge-Kutta method, a cubic one for a fourth order Runge-Kutta method. However, if the change of the interaction term when a neuron fires a new spike is not carefully taken into account when computing the new value of the potential, an error of order $O(\Delta t^2)$, inconsistent with any RK algorithm of order higher than 2, is introduced. One way to avoid this problem is to adopt an adaptive time step at firing times but the computation time is then dominated for large time steps by the determination of the firing times, which depends little on Δt . As a consequence, higher order algorithms are less efficient than the RK2I scheme. For instance, the RK2I algorithm with a time step of 0.1 ms always leads over the RK3I algorithm by a factor of at least 2.5. This shows that among Runge-Kutta algorithms, the RK2I scheme is optimal for integrating the deterministic dynamics of IF networks.

Finally we discuss the respective effects of the two types of error of order $O(\Delta t)$ exhibited by standard algorithms (see section 3.1.3). The first error originates in the single cell dynamics and does not occur in the smooth dynamics of conductance-based models. It is linked to the behavior of the

potential at firing times and is present even if the membrane potential is continuous at firing times. An example is provided by a frequently employed type of IF neuron, where the smooth repolarization of the membrane potential is due to an “AHP current” turned on by the spikes of the neuron:

$$I_{AHP}(t) = -g_{AHP}(V - V_{AHP}) \sum_{\text{spikes of the neuron}} g(t - t_{\text{spike}}) \quad (28)$$

Here $g(t)$ is an “alpha function” with a time constant t_{AHP} , and V_{AHP} is the reversal potential. The membrane potential and its first derivative are then continuous but its second derivative is discontinuous at firing times. The error at each time step is of order $O(\Delta t^2)$ but it accumulates over time and still leads to a global error of order $O(\Delta t)$. Here again, the problem can be corrected by an interpolation scheme.

The second error of order $O(\Delta t)$ occurs only in networks and is mediated by the interaction between neurons. It is caused by errors in the determination of spiking times, is not related to the precise form of the interaction, and is present whenever firing times are determined by the crossing of a threshold. This form of discontinuity in the dynamics is present for networks of conductance based model when an “ α function” is used to model the synaptic interactions. The classical Runge-Kutta schemes (Euler, RK2 ...) are all first order in that case but one can devise a really second order Runge Kutta scheme by determining firing times via a linear interpolation.

Higher order schemes can also be implemented but they are more costly in terms of computation time and the RK2I method again appears to be optimal. However the maximum time step is now fixed by the steepness of the problem, that is, by the rise time of spikes. This maximal time step is of the order of 0.05 ms , which strongly limits the gains obtained from the use of the RK2I algorithm as the standard methods allow one to estimate the coherence within a few percents for such a time step. The error mediated by the interaction is expected to have no major consequences on the dynamics of conductance-based models in that range of time steps.

All the results presented in this paper concern deterministic models. Issues similar to those investigated in the present study need to be studied when noise is also present in the network dynamics, and will be addressed in a subsequent work.

Acknowledgements

We are thankful to C. Van Vreeswijk for most helpful discussions. We thank D. Golomb and C. Van Vreeswijk for careful reading of the manuscript. D.H. and L.N. acknowledge the very warm

hospitality of the Center for Neural Computation and the Racah Institute of Physics of the Hebrew University where part of this work was done. The work of L.N. was partially supported by the DRET. G.M. thanks the Spanish Ministry of Education and Science for financial support. Part of the numerical simulations have been performed on the CRAY C90 of IDRIS (Orsay, France).

5 Appendix

Let us suppose that $V(t) < \theta$ and $V_0(t+\Delta t) \geq \theta$. Using Eq. (17), one evaluates by linear interpolation the time t_{sp} ($t < t_{sp} < t + \Delta t$) at which the membrane potential reaches the threshold :

$$t_{sp} = t + \Delta t \frac{\theta - V(t)}{V_0(t + \Delta t) - V(t)} \quad (29)$$

The membrane potential is reset to V_{rest} at that time. Between t_{sp} and $t + \Delta t$ the time derivative of the membrane potential is given at lowest order by

$$\frac{dV}{dt}(t_{sp}) = \frac{dV}{dt}(t) + g_l(V(t) - V_{rest}) = \frac{V_0(t + \Delta t) - V(t)}{\Delta t} + g_l(V(t) - V_{rest}) \quad (30)$$

$V(t + \Delta t)$ is equal at the order considered to $V(t_{sp}) + (t + \Delta t - t_{sp})\frac{dV}{dt}$. Using this equation and the estimated value of t_{sp} , one gets Eq. (20). The synaptic current is updated at time $t + \Delta t$ using the firing time of Eq. (29). We do not take into account the change in the synaptic current in the time interval $[t, t + \Delta t]$ due to the firing at time t_{sp} since doing it consistently requires to determine which neuron fires first and to adopt an adaptive time step. This would increase significantly the computation time. The global error associated with this approximation is of order $O(\Delta t^2)$ and thus consistent with the improved versions of the Euler and RK2 algorithms.

REFERENCES

- Ginzburg, I., and Sompolinsky, H. 1994, Theory of correlations in stochastic neural networks. *Phys. Rev.*, **E50**, 3171-3191.
- Golomb, D., and Rinzel, J. 1993, Dynamics of globally coupled inhibitory neurons with heterogeneity. *Phys. Rev. E*, **48**, 4810-4814.
- Hansel, D., and Sompolinsky, H. 1992, Synchronization and computation in a chaotic neural network. *Phys. Rev. Lett.* **68**, 718-721.
- Hansel, D., Mato, G., and Meunier, M. 1995, Synchrony in excitatory neural network. *Neural Comp.*, **7**, 307-337.
- Hansel, D., and Sompolinsky, H. 1996, Chaos and synchrony in a model of a hypercolumn in visual cortex. *J. Comp. Neurosci.*, **3**, 7-34.
- Hodgkin, A.L., and Huxley, A.F. 1952, A quantitative description of membrane current and its application to conduction and excitation nerve. *J. Physiol. (London)* **117**, 500-544.
- Lapicque, L. 1907. Recherches quantitatives sur l'excitation électrique des nerfs traitée comme une polarisation. *J. Physiol. Pathol. Gen.*, **9**, 620-635.
- Mascagni, M.V. and Sherman, A. 1997, *Numerical methods for neural modeling*. In Methods in Neuronal Modeling. From Synapses to Networks, C. Koch, and I. Segev, second edition. MIT Press, Cambridge, MA. To appear.
- Tsodyks, M., Mitkov, I., and Sompolinsky, H. 1993, Patterns of synchrony in integrate-and-fire network. *Phys. Rev. Lett.* **71**, 1280-1283.
- Tuckwell, H.C. 1988, *Introduction to theoretical neurobiology*. Cambridge University Press, Cambridge.
- Van Vreeswijk C., Abbott, L.F., Ermentrout, G.B., 1995, Inhibition, not excitation synchronizes coupled neurons. *J. Comp. Neurosci.*, **1**, 313-321.

Wehmeir, U., Dong D., Koch, C., and Van Essen, D. 1989, *Modeling the Mammalian Visual System*.
In Methods in Neuronal Modeling. From Synapses to Networks, C. Koch, and I. Segev, eds,
pp. 335-359. MIT Press, Cambridge, MA.

Method	time step (ms) for 10% on ϵ_t	time step (ms) for 1% on ϵ_t
Standard Euler	$2.4 \cdot 10^{-4}$	$3.0 \cdot 10^{-5}$
Euler with interpolation	$4.9 \cdot 10^{-4}$	$6.1 \cdot 10^{-5}$
Standard RK2	$9.8 \cdot 10^{-4}$	$1.2 \cdot 10^{-4}$
RK2 with interpolation	$3.1 \cdot 10^{-2}$	$7.8 \cdot 10^{-3}$

Table 1: The maximum time step allowed for the four methods to get a 10% and 1% precision on ϵ_t . Same network parameters as in Fig. 3.

Method	time step (ms) for 10% on Σ	time step (ms) for 1% on Σ
Standard Euler	$3.1 \cdot 10^{-2}$	$2.0 \cdot 10^{-3}$
Euler with interpolation	$6.2 \cdot 10^{-2}$	$2.0 \cdot 10^{-3}$
Standard RK2	$6.2 \cdot 10^{-2}$	$3.9 \cdot 10^{-3}$
RK2 with interpolation	0.25	$6.3 \cdot 10^{-2}$

Table 2: The maximum time step allowed for the four methods to get a 10% and 1% precision on the coherence Σ . Same network parameters as in Fig. 3.

Method	CPU per time step (s)
Standard Euler	$4.6 \cdot 10^{-5}$
Euler with interpolation	$4.8 \cdot 10^{-5}$
Standard RK2	$8.1 \cdot 10^{-5}$
RK2 with interpolation	$8.6 \cdot 10^{-5}$

Table 3: The CPU time per time step for the four integration schemes used.

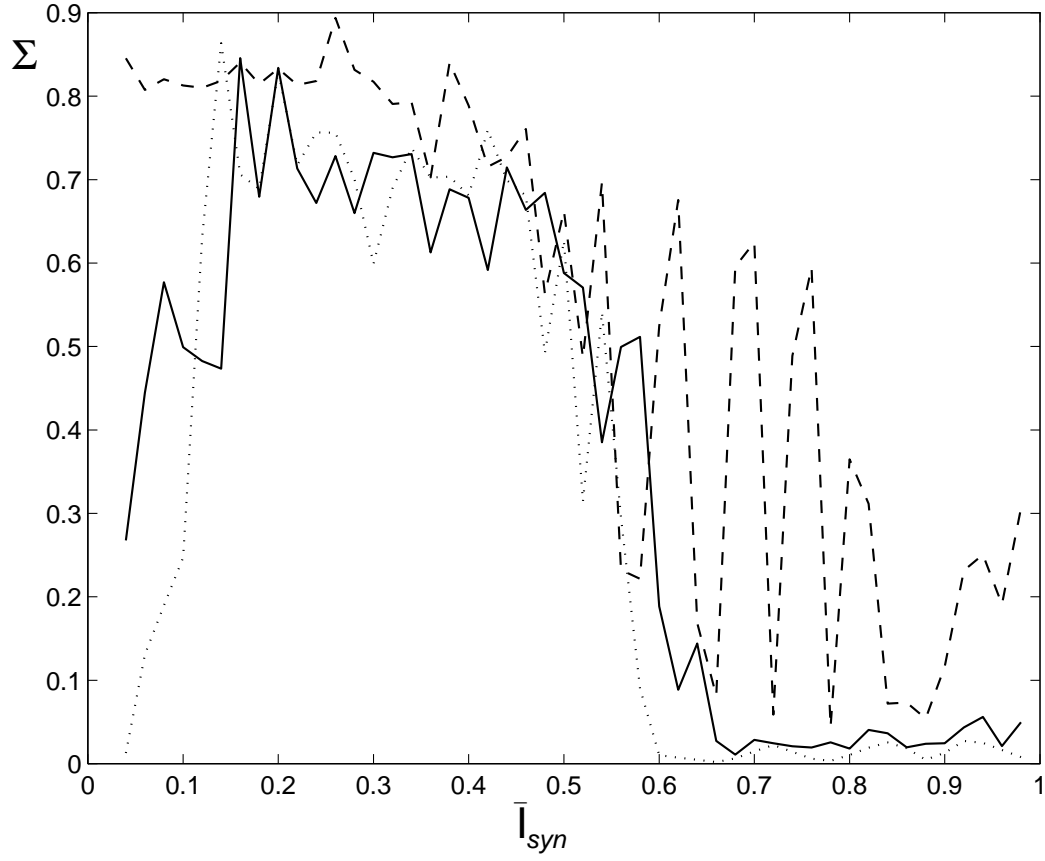


Figure 1: Coherence Σ as a function of the coupling strength \bar{I}_{syn} ($\mu A/cm^2$) for the Euler algorithm and different time steps: Dashed line: $\Delta t = 0.25$ ms; Dotted line: $\Delta t = 0.1$ ms; Dashed-dotted line: $\Delta t = 0.01$ ms; Full line: Exact integration.

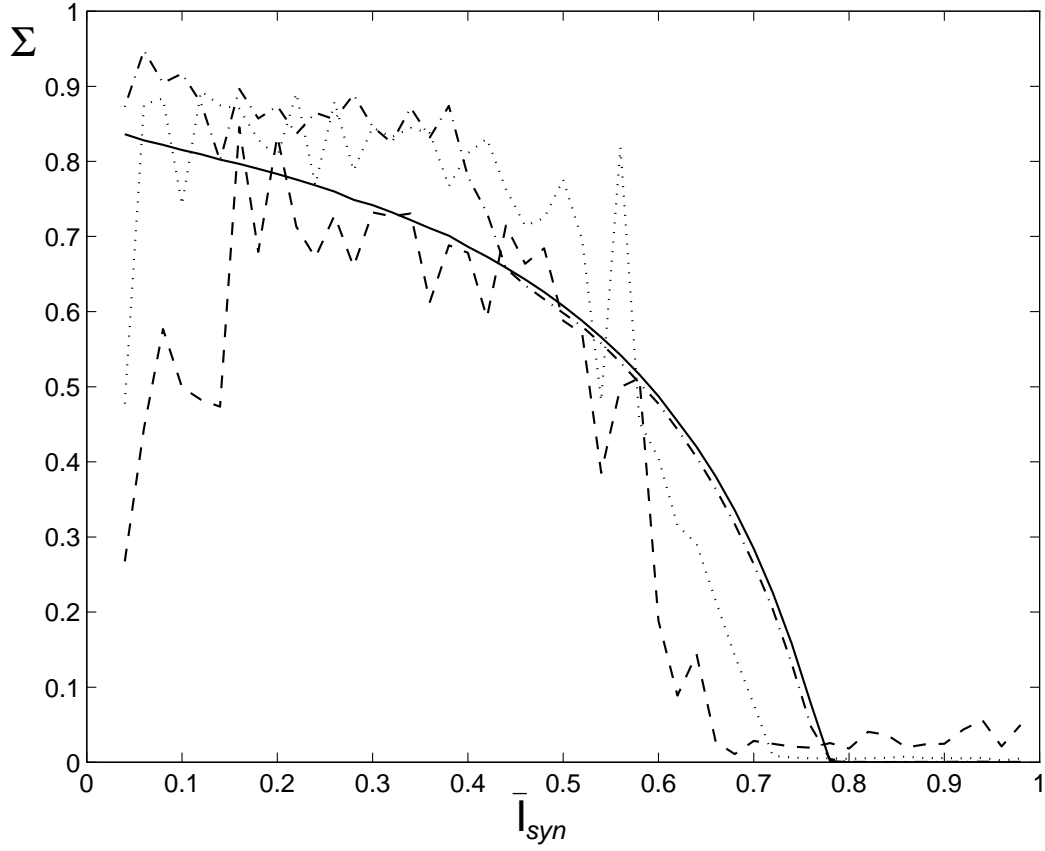


Figure 2: Coherence Σ as a function of the coupling strength \bar{I}_{syn} ($\mu A/cm^2$) for the Euler algorithm ($\Delta t = 0.25$ ms) and different initial conditions: Dashed line: $c = 0.1$; Full line: $c = 0.5$; Dotted line: $c = 0.9$.

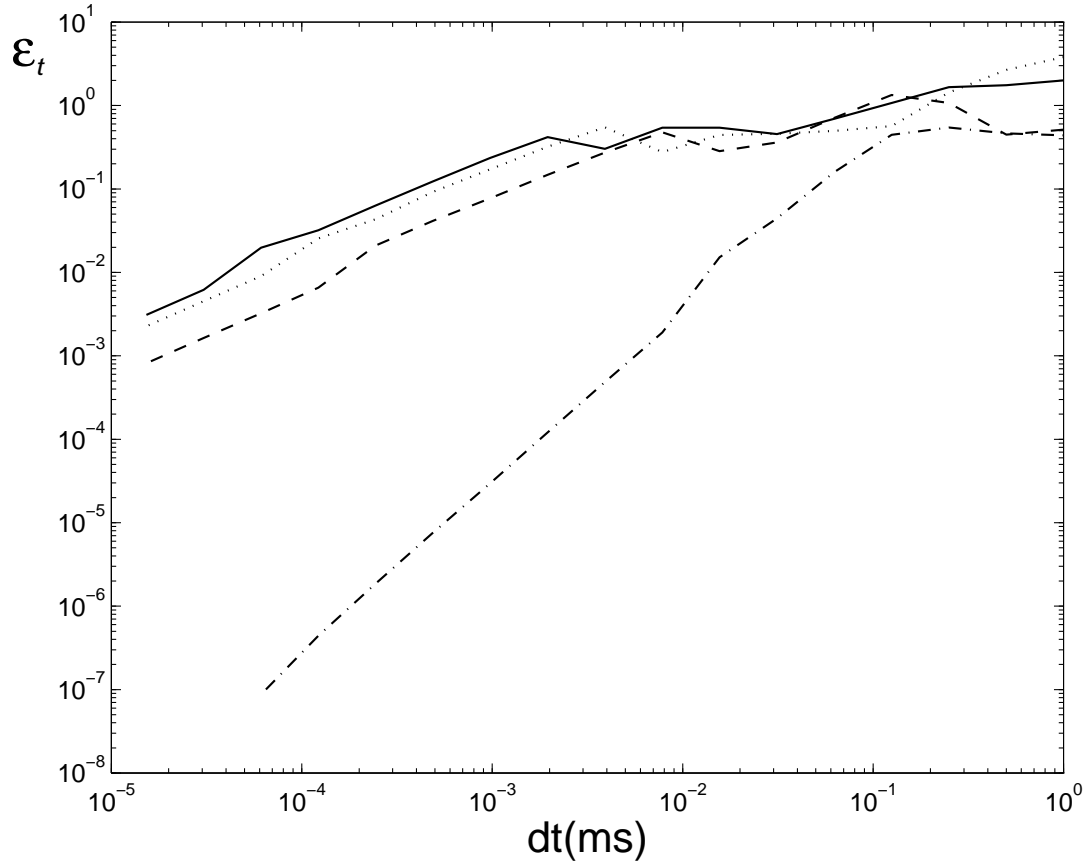


Figure 3: Relative error on the firing times ϵ_t as a function of the time step for the different algorithms: Full line: standard Euler; Dotted line: Euler with interpolation; Dashed line: Standard RK2; Dashed-dotted RK2 with interpolation.

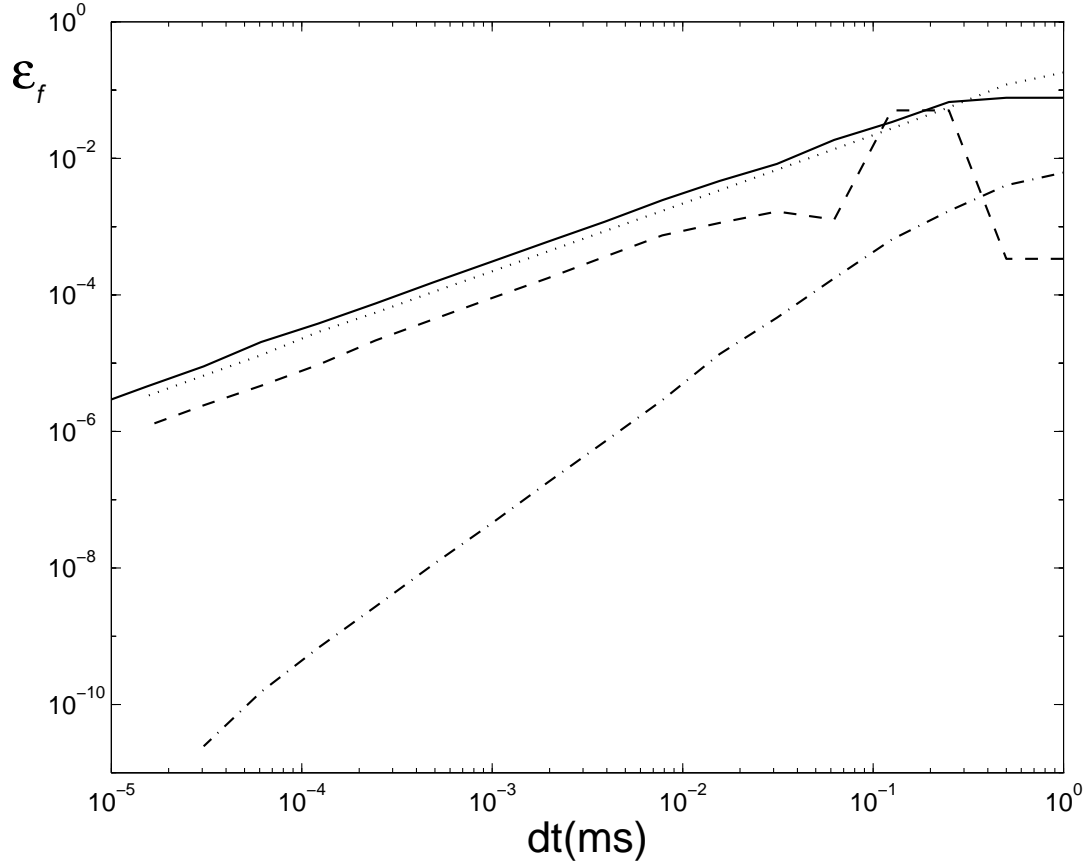


Figure 4: Relative error on the firing rate ϵ_f as a function of the time step for the different algorithms. Same conventions as in Fig. 3.

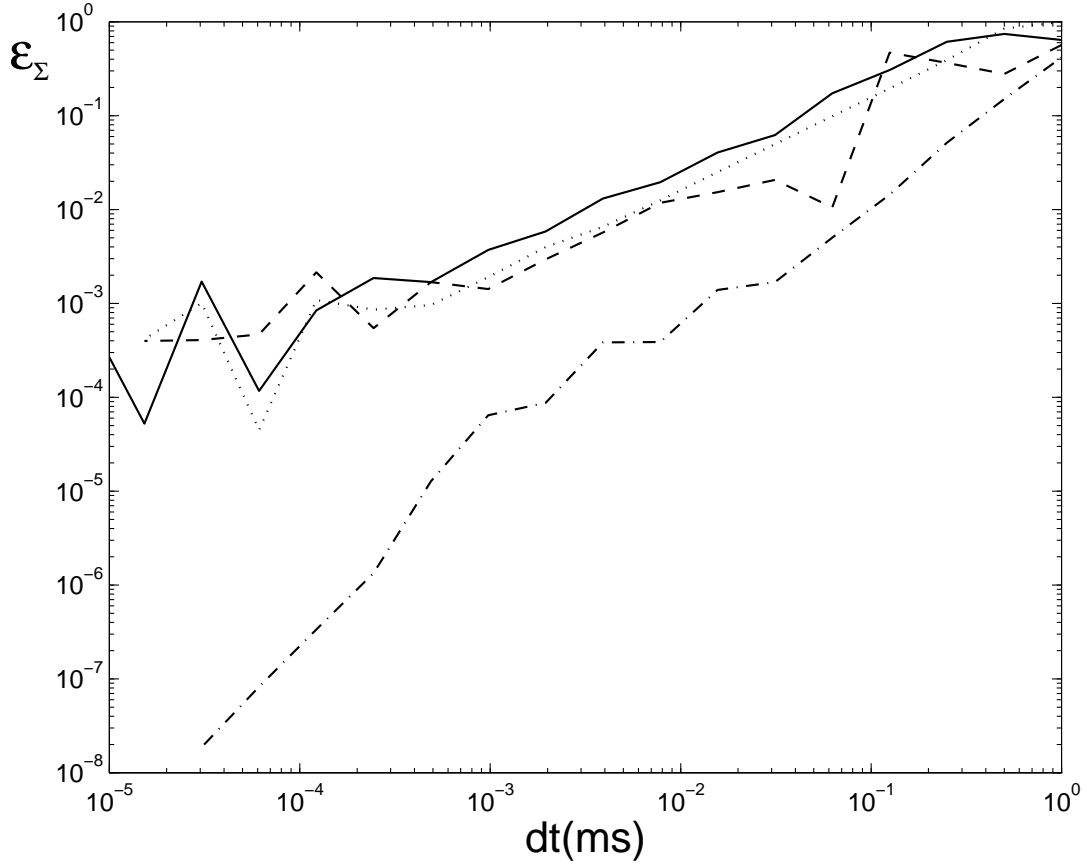


Figure 5: Relative error on the coherence ϵ_Σ as a function of the time step for the different algorithms. Same conventions as in Fig. 3.

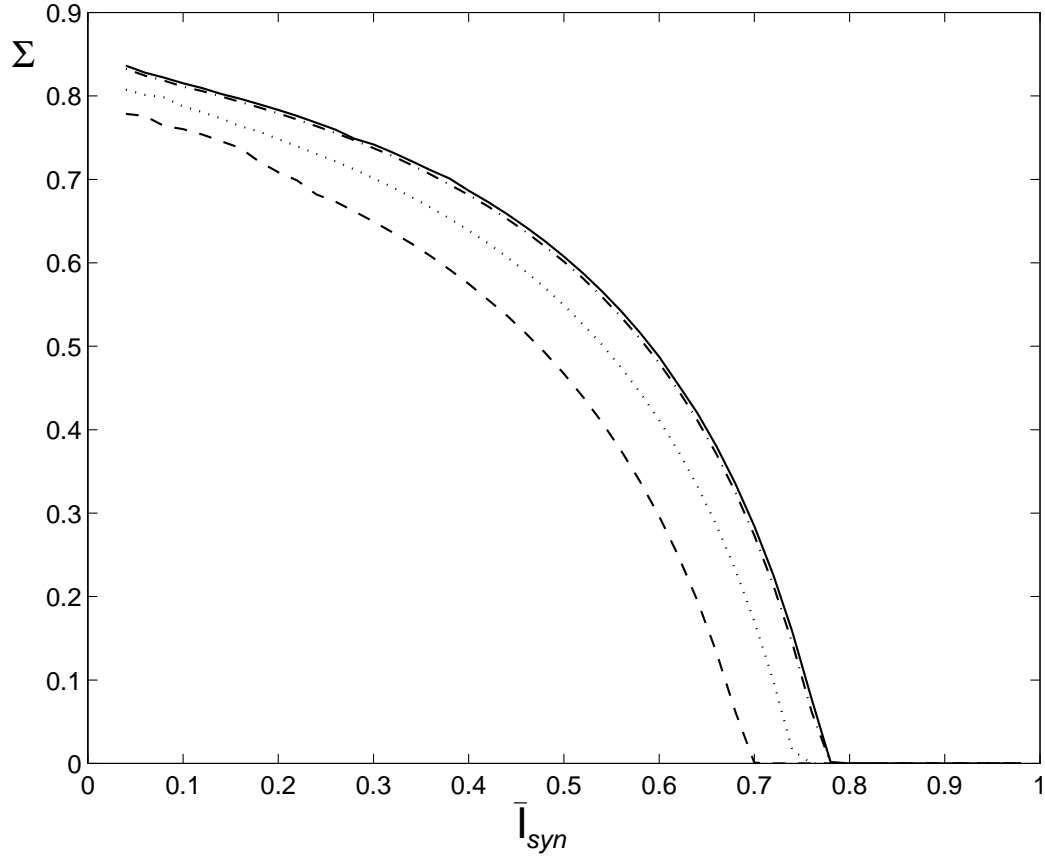


Figure 6: Coherence Σ as a function of the coupling strength \bar{I}_{syn} ($\mu A/cm^2$) for the modified Euler algorithm and different time steps. Same conventions as in Fig. 1.

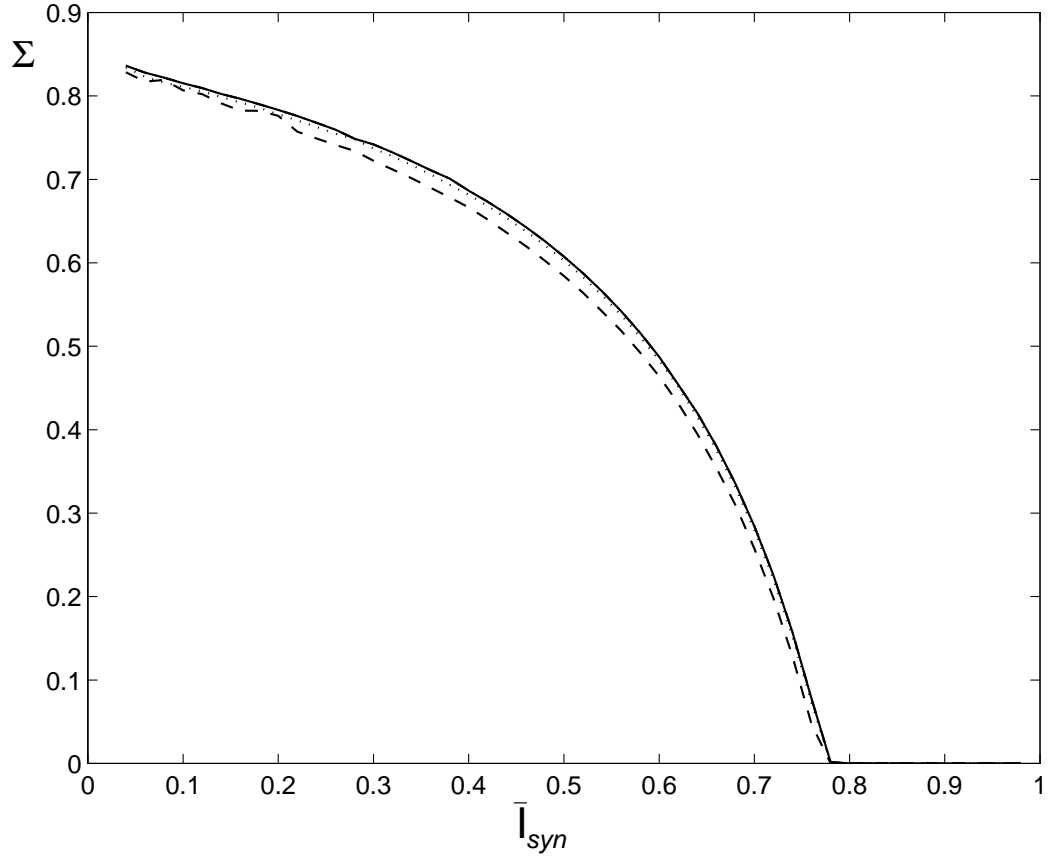


Figure 7: Coherence Σ as a function of the coupling strength \bar{I}_{syn} ($\mu A/cm^2$) for the modified RK2 and different time steps. Same conventions as in Fig. 1.